# Switchable Mesomorphic Materials Based on the Ferrocene−Ferrocenium Redox System: Electron-Transfer-Generated Columnar Liquid-Crystalline Phases

Robert Deschenaux,* Martin Schweissguth, and Maria-Teresa Vilches

*Institut de Chimie, Université de Neuchâtel, Avenue de Bellevaux 51, 2000 Neuchâtel, Switzerland*

Anne-Marie Levelut*

*Laboratoire de Physique des Solides, Université Paris-Sud, Bâtiment 510, 91405 Orsay Cedex, France*

Dimitri Hautot and Gary J. Long*

*Department of Chemistry, University of Missouri−Rolla, Rolla, Missouri 65409-0010*

Dominique Luneau*

*Laboratoire de Chimie de Coordination, Service de Chimie Inorganique et Biologique, Département de Recherche Fondamentale sur la Matière Condensée, Commissariat à l'Energie Atomique, 17 Rue des Martyrs, 38054 Grenoble Cedex, France*

*Received July 12, 1999*



Oxidation of the non-mesomorphic ferrocene derivative **1** with silver toluene-4-sulfonate gave the ferrocenium derivative **2**, which showed a monotropic columnar phase. The latter two-dimensional phase is composed of ribbons, in which derivative **2** is organized into bilayers, and has a centered rectangular symmetry with $a = 318.3$ Å and $c = 94.9$ Å. The Mössbauer spectra of the ferrocene derivative **1** yields hyperfine parameters that are typical of these derivatives and are, as expected, virtually independent of temperature. In a similar fashion, the hyperfine parameters of the ferrocenium derivative **2** are typical of these derivatives, but in this case at both 78 and 4.2 K slow paramagnetic relaxation of the magnetic moment associated with the rather well isolated paramagnetic ferrocenium ion is observed. The temperature-dependent magnetic susceptibilities of **2** are in agreement with those expected for weakly interacting ferrocenium cores. No magnetic-field-induced orientation was observed upon cooling the sample from the isotropic phase down to the columnar phase. Ferrocene and ferrocenium are valuable units for the design of liquid-crystalline switches.

## Introduction

Recently, we reported the first evidence that the ferrocene−ferrocenium redox system can be used to prepare switchable liquid crystals (Chart 1):[1] although the ferrocene derivative **I** was non-mesomorphic, its oxidized form **II** gave rise to a monotropic smectic A phase. A peralkylated ferrocene was selected as the redox-active center in order to utilize the ease of the oxidation process of this unit in comparison with less alkylated ferrocenes.[2]

The mesomorphic properties of ferrocene-containing thermotropic liquid crystals depend on the nature, number, and position of the substituents located on the ferrocene:[3] (1) polycatenar ferrocene derivatives gave columnar liquid-crystalline phases,[4] (2) functionalization of ferrocene with flexible chains led to mesomorphism near room temperature,[5] and (3) 1,3-disubstituted ferrocene derivatives had a greater tendency to form liquid-crystalline phases than their 1,1′-isomeric analogues.[6] Therefore, we anticipated that the system described in Chart 1 reflected only one particular switching mode and that modification of the organic entity connected to the ferrocene nucleus would lead to different situations: other possibilities are the switching

(1) Deschenaux, R.; Schweissguth, M.; Levelut, A.-M. *Chem. Commun.* **1996**, 1275.
(2) Zanello, P. In *Ferrocenes: Homogeneous Catalysis, Organic Synthesis, Materials Science;* Togni, A., Hayashi, T., Eds.; VCH: Weinheim, Germany, 1995; Chapter 7.
(3) Deschenaux, R.; Goodby, J. W. In *Ferrocenes: Homogeneous Catalysis, Organic Synthesis, Materials Science;* Togni, A., Hayashi, T., Eds.; VCH: Weinheim, Germany, 1995; Chapter 9.
(4) Deschenaux, R.; Monnet, F.; Serrano, E.; Turpin, F.; Levelut, A.-M. *Helv. Chim. Acta* **1998**, *81*, 2072.
(5) Deschenaux, R.; Turpin, F.; Guillon, D. *Macromolecules* **1997**, *30*, 3759.
(6) Deschenaux, R.; Marendaz, J.-L. *J. Chem. Soc., Chem. Commun.* **1991**, 909.

10.1021/om9905308 CCC: $18.00 
Publication on Web 12/02/1999

**Chart 1**

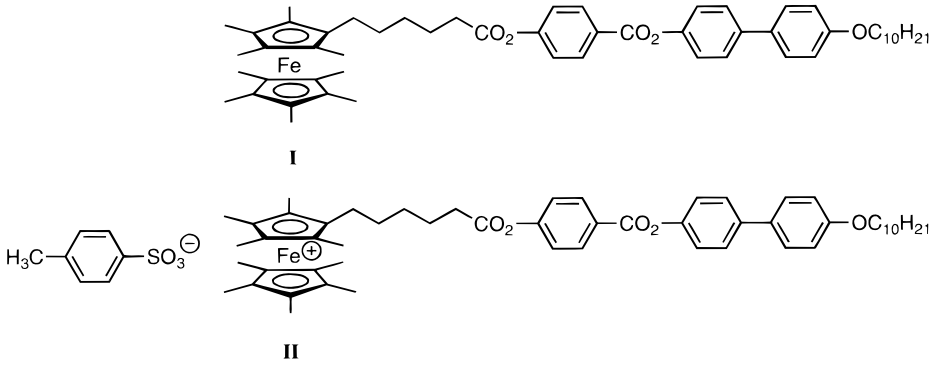


**Chart 2**

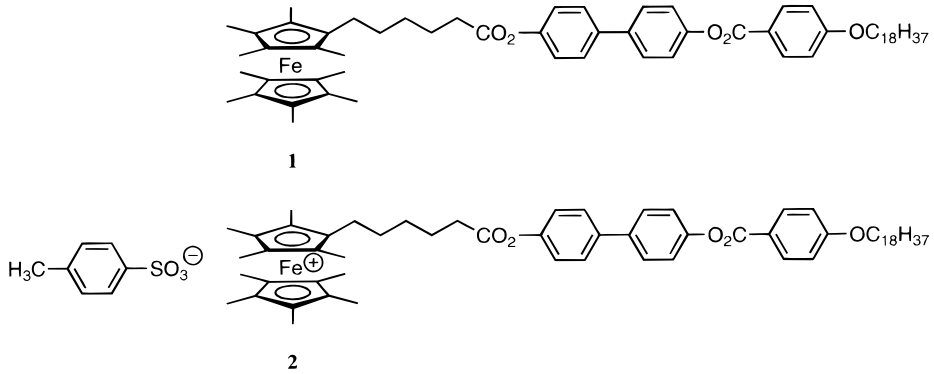




from a mesomorphic ferrocene to a non-mesomorphic ferrocenium (the reverse sequence from that presented in Chart 1) or between mesomorphic ferrocene and ferrocenium derivatives, each of them giving rise to different liquid-crystalline phases.

The ultimate objective of our research is the design of ferrocene-based switchable liquid crystals with tailor-made properties. To reach this goal, an understanding of the structural factors (number of aromatic rings in the rigid rod, length of the terminal alkyl chain, length of the spacer between the ferrocene and the rigid segment, nature of the counterion) which govern the mesomorphism is essential and requires the design and study of further structures.

We report, herein, the synthesis, liquid-crystalline, Mössbauer spectral, and magnetic properties of compounds **1** and **2** (Chart 2) which form a new mesogenic redox-active couple. In comparison with **I** and **II**, a longer alkyl chain was used to functionalize the promesogenic organic rod (18 carbon atoms instead of 10). The purpose of this change was to explore the possibility of obtaining other liquid-crystalline phases than that observed for **II**. In **1** and **2**, the three aromatic rings are connected differently than in **I** and **II**. This modification was applied only for synthetic purposes, such as ease of purification of the intermediates, and was not expected to influence markedly the thermal and mesomorphic properties of the resulting compounds.

## Results and Discussion

**Synthesis.** The preparation of **1** and **2** is described in Scheme 1. Treatment of nonamethylferrocene carboxaldehyde[7] (**3**) with (4-carboxybutyl)triphenylphosphonium bromide under Wittig reaction conditions gave **4**. Esterification of **4** with 4-benzyloxy-4′-hydroxybiphenyl[8] yielded **5**. Reduction of the carbon−carbon double bond and removal of the benzyl protected group was accomplished under hydrogenation reaction conditions and gave **6**, which, when condensed with 4-octadecyloxybenzoic acid,[9] led to the expected ferrocene derivative **1**. Oxidation of **1** with silver toluene-4-sulfonate yielded the ferrocenium species **2**.

**Table 1. Phase Transitions of Compounds 1 and 2**

| compound | phase transition[a] | *T*, K | Δ*H*, kJ/mol |
|---|---|---|---|
| **1** | Cr → I | 407[b] | 55 |
| **2** | Cr → I | 396[b] | 81 |
| | (I → $Col_{rect}$)[c] | 374[d] | *e* |

[a] Cr = crystalline state, I = isotropic liquid, $Col_{rect}$ = rectangular columnar phase. [b] Onset transition determined by DSC during the first heating run. [c] Monotropic transition. [d] Determined by polarized optical microscopy. [e] Not detected; see main text for details.

**Liquid-Crystalline Properties.** The thermal and liquid-crystalline behavior of **1** and **2** were examined by polarized optical microscopy (POM), differential scanning calorimetry (DSC), and X-ray diffraction (XRD). The thermal and liquid-crystalline results are listed in Table 1.

No liquid-crystalline properties were observed for **1**. The unique event that was detected is the melting of the sample into an isotropic melt.

(7) Kreindlin, A. Z.; Fadeeva, S. S.; Rybinskaya, M. I. *Izv. Akad. Nauk SSSR, Ser. Khim.* **1984**, 403.
(8) (a) Shedouda, I. G.; Shi, Y.; Neubert, M. E. *Mol. Cryst. Liq. Cryst.* **1994**, *257*, 209. (b) Bruce, J. M.; Chaudhry, A. *J. Chem. Soc., Perkin Trans. 1* **1974**, 295.
(9) Deschenaux, R.; Marendaz, J.-L., Santiago, J. *Helv. Chim. Acta* **1993**, *76*, 865.

**Scheme 1**[a]

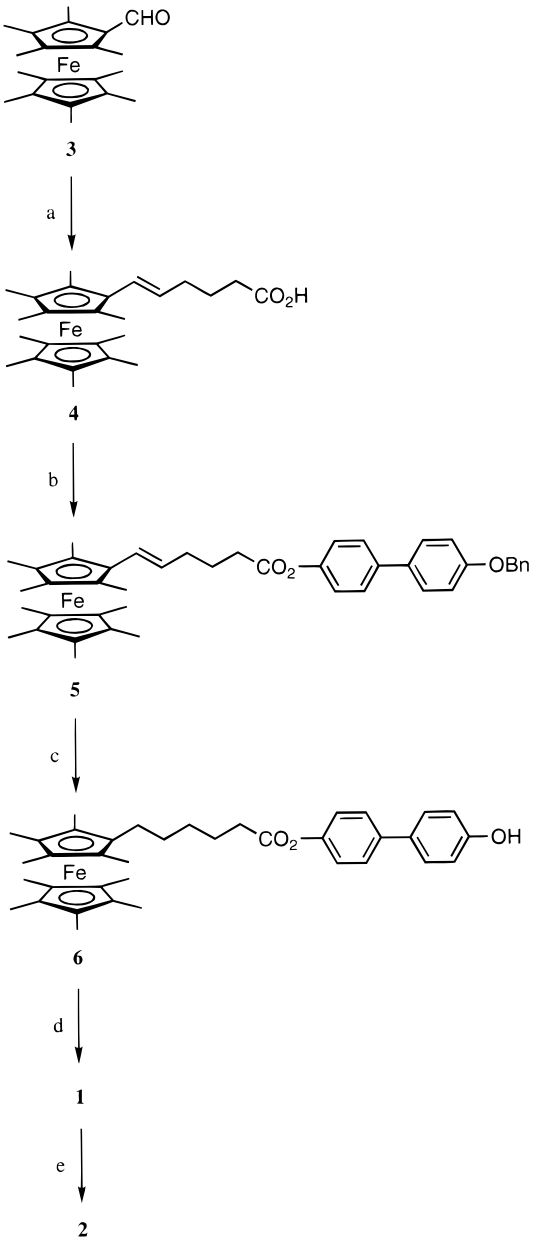


[a] Key: (a) (4-carboxybutyl)triphenylphosphonium bromide, $^t$BuOK, THF, 84%; (b) 4-benzyloxy-4′-hydroxybiphenyl, *N*,*N*′-dicyclohexylcarbodiimide (DCC), 4-pyrrolidinopyridine, $CH_2Cl_2$, 77%; (c) $H_2$, Pd/C, $CH_2Cl_2$, 78%; (d) 4-octadecyloxybenzoic acid, *N*,*N*′-dicyclohexylcarbodiimide (DCC), 4-pyrrolidinopyridine, $CH_2Cl_2$, 69%; (e) silver toluene-4-sulfonate, $CH_2Cl_2$/acetone, 78%. All the reactions were carried out at room temperature.

Upon heating, compound **2** melted into an isotropic fluid, and the formation of a columnar liquid-crystalline phase was observed at 374 K by POM when the sample was cooled from the isotropic melt. The mesophase was identified from its optical texture, which is typical for columnar liquid-crystalline phases (Figure 1). As a consequence of a very small enthalpy change, no exothermic peak was detected by DSC at 374 K. Such an observation has already been reported for columnar-to-isotropic fluid phase transition.[10] Further cooling led to a modification of the texture at 364 K. This transformation could not be identified by POM.

(10) Kang, S. H.; Kim, M.; Lee, H.-K.; Kang, Y.-S.; Zin, W.-C.; Kim, K. *Chem. Commun.* **1999**, 93.

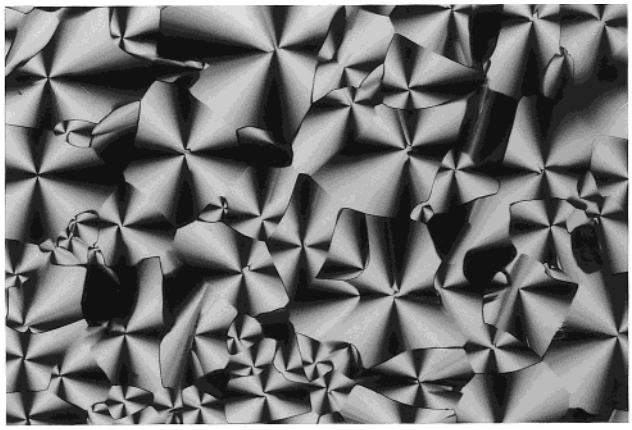

**Figure 1.** Texture of the rectangular columnar phase displayed by **1** upon cooling slowly the sample from the isotropic liquid to 374 K.

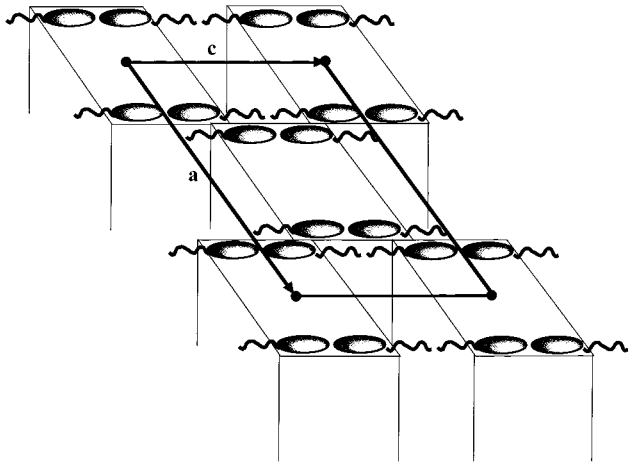


**Figure 2.** Schematic representation of the columnar rectangular liquid-crystalline phase.

**Table 2. Observed and Calculated *d* Spacings (Å) of the Liquid-Crystalline Phase of Compound 2**[a]

| *h* | *k* | *l* | $d_{obs}$ | $d_{calc}$ |
|---|---|---|---|---|
| 2 | 0 | 0 | 158.5 | 159.1 |
| 1 | 0 | 1 | 90.2 | 91.2 |
| 4 | 0 | 0 | 79.2 | 79.6 |
| 3 | 0 | 1 | 70.7 | 70.8 |
| 6 | 0 | 0 | | 53.1 |
| 5 | 0 | 1 | | 52.7 |
| 0 | 0 | 2 | 47.6 | 47.5 |
| 5 | 0 | 5 | 18.4 | 18.2 |

[a] The lattice is centered rectangular ($a$ = 318.3 Å and $c$ = 94.9 Å). Between the 002 and the last observed Bragg reflection there are several unobserved reflections.

The columnar nature of the liquid-crystalline phase was established by XRD. The structure of the phase is shown in Figure 2, and the XRD data are collected in Table 2.

The unit cell of this two-dimensional phase has a centered rectangular symmetry of dimensions 318.3 Å × 94.9 Å. By Corey−Pauling−Koltun (CPK) space-filling molecular models, an approximate molecular length of 51 Å was obtained for **1** in the fully extended conformation. Therefore, there are two molecules within the thickness of the ribbons, an organization that corre-

sponds to a bilayer. The total length of two aligned molecules ($2 \times 51 = 102$ Å) is larger than the thickness of the ribbon (94.9 Å). The discrepancy between both values (i.e., 102 and 94.9 Å) indicates that the molecules are slightly interdigitated and/or not in a fully elongated conformation. The ribbons are disposed in staggered rows. Constraint of curvatures due to the difference of molecular areas between the ferrocene unit and the paraffinic chain is probably responsible for the formation of columns.[11]

XRD measurements were also recorded at 363 K. At this temperature, the diffraction pattern revealed the formation of a crystalline structure. Therefore, the modification observed by POM at 364 K reflected solidification of the sample.

The fragility of the sample at elevated temperature and under X-ray irradiation was revealed by XRD, which indicated that the columns degraded into lamellae (i.e., the columnar phase transformed into a fluid lamellar phase); the layer periodicity decreased by about 10% (from 94.9 Å to ca. 85 Å) within 1 h.

The results obtained for **1** and **2** can be rationalized on the basis of structural considerations. The nonmesomorphic character of **1** is the consequence of the presence of the bulky alkylated ferrocene unit, a unit that decreases the intermolecular interactions[3] responsible for generating mesomorphism. This interpretation is supported by results we recently obtained: an increase in the length of the promesogenic rod (four aromatic rings instead of three) led to materials showing enantiotropic liquid-crystalline behavior.[12] The mesomorphic character of **2** proves that ionic interactions play an important role in inducing mesomorphism. Finally, the monotropic nature of the liquid-crystalline phase exhibited by **2** also results from the presence of the bulky alkylated ferrocene which reduces the intermolecular interactions as for **1**.

**Mössbauer Spectroscopy.** The Mössbauer spectra can be divided into two groups: the unoxidized species and the oxidized material. The first group of spectra all exhibit a simple quadrupole doublet, as is shown in Figure 3 for **1**. These spectra have been fit with the same linewidth for each component of the doublet, but in some cases, the relative areas of the two components differed by a few percent, presumably as a result of texture. The resulting spectra and the spectral hyperfine parameters, which are given in Table 3, are typical of those observed[13] for $Cp_2Fe$ and its derivatives. However, it should be noted that the isomer shifts, $\delta$, of $(Me_5Cp)_2Fe$ are slightly lower than those of $Cp_2Fe$. The lower values correspond to a higher s-electron density at the iron nucleus in $(Me_5Cp)_2Fe$ as a consequence of the additional stability associated with its stronger bonding as compared to $Cp_2Fe$. In contrast, the observed isomer shifts for $(Me_5Cp)_2Fe$ and its derivative **1** are, as expected, essentially identical within experimental error, and the presence of the mesogenic framework has little influence upon the bonding at the iron site.

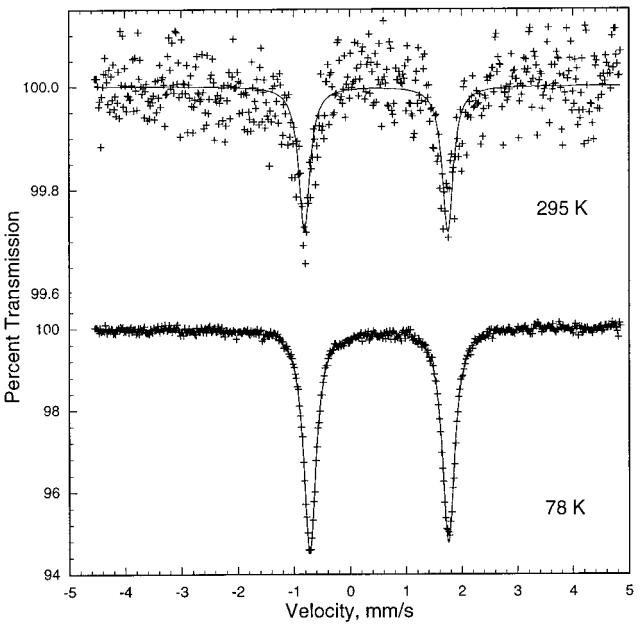


**Figure 3.** Mössbauer effect spectra of **1**.

**Table 3. Mössbauer Spectral Parameters of $Cp_2Fe$, $(Me_5Cp)_2Fe$, and 1**

| compound | $T$, K | $\delta$, mm/s[a] | $\Delta E_Q$, mm/s | $\Gamma$, mm/s | $M_{eff}$, g/mol | $\Theta_D$, K |
|---|---|---|---|---|---|---|
| $Cp_2Fe$ | 295 | 0.447 | 2.40 | 0.23 | 101[b] | 94[b] |
| | 85 | 0.533 | 2.40 | 0.26 | | |
| $(Me_5Cp)_2Fe$ | 295 | 0.428(4) | 2.48(2) | 0.23(1) | 104[b] | 88[b] |
| | 85 | 0.503 | 2.48 | 0.25 | | |
| **1** | 295 | 0.434 | 2.44 | 0.24 | 129 | 71 |
| | 78 | 0.504 | 2.46 | 0.24 | | |

[a] The isomer shifts are reported relative to room temperature α-iron foil. [b] Obtained from ref 15.

However, the mesogenic framework does make small, but probably real, differences in the local site symmetry at the iron, as is reflected in the small differences in the quadrupole splittings, $\Delta E_Q$.

By studying the temperature dependence of the Mössbauer spectral isomer shifts and absorption areas, it is possible to determine[14] the effective recoil mass, $M_{eff}$, and the effective Mössbauer temperature, $\Theta_D$, of an iron-containing compound. The effective recoil mass is a measure of the covalency of the iron bonding, whereas the effective Mössbauer temperature is equivalent to the Debye temperature of an element. These measurements have been carried out earlier[15] for $Cp_2Fe$ and $(Me_5Cp)_2Fe$, and the resulting values are given in Table 3. The equivalent values for **1** are also given in Table 3, although in this case the results are based on only two data points and thus are more uncertain. The observed values do seem to indicate a higher covalency and a smaller Mössbauer temperature for **1** as compared to $Cp_2Fe$ and $(Me_5Cp)_2Fe$.

The Mössbauer spectra of the oxidized compound **2** (Figure 4) are quite different from those of the unoxidized species. At 295 K, only one line is observed, and as expected, the large quadrupole splitting of the $(Me_5Cp)_2Fe$ derivatives has collapsed to virtually zero. If the 295 K spectra is measured over a reduced velocity range,

(11) (a) Hendrikx, Y.; Levelut, A.-M. *Mol. Cryst. Liq. Cryst.* **1988**, *165*, 233. (b) Sigaud, G.; Hardouin, F.; Achard, M. F.; Levelut, A.-M. *J. Physique* **1981**, *42*, 107.

(12) Deschenaux, R.; Schweissguth, M.; Vilches, M.-T. Unpublished results.

(13) Parish, R. V. In *The Organic Chemistry of Iron*; Koerner von Gustorf, E. A., Grevels, F., Fischler, I., Eds.; Academic Press: New York, 1978; Vol. 1, p 192.

(14) Earnst, R. D.; Wilson, D. R.; Herber, R. H. *J. Am. Chem. Soc.* **1984**, *106*, 1646.

(15) Long, G. J. Unpublished results.

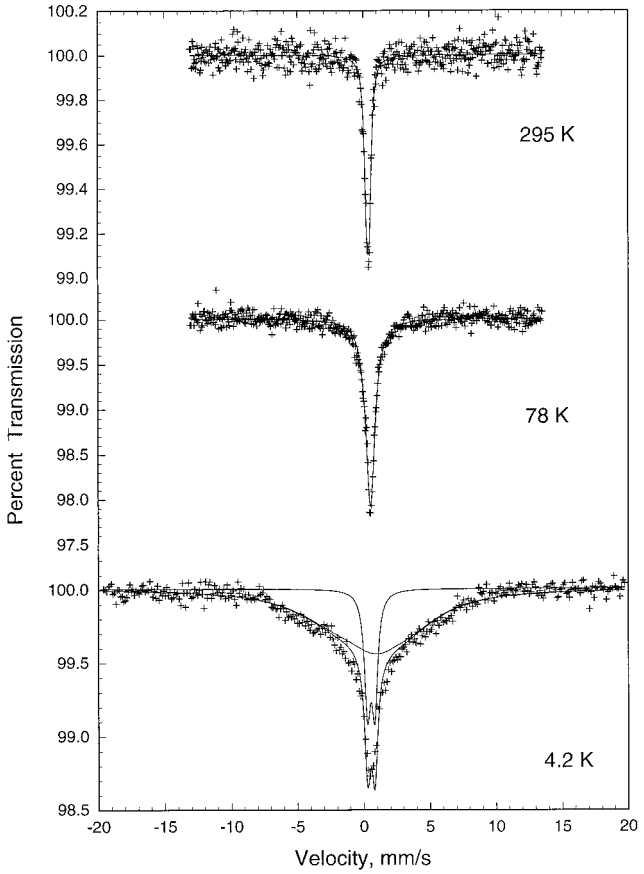


**Figure 4.** Mössbauer effect spectra of **2**.

**Table 4. Mössbauer Spectral Parameters of Compound 2**

| $T$, K | $\langle H_{eff} \rangle$, kOe | $\delta$, mm/s[a] | $\Delta E_Q$, mm/s | $\Gamma$, mm/s |
|---|---|---|---|---|
| 295 | 0 | 0.38 | 0.26 | 0.36 |
| 78 | 13 | 0.47 | | |
| 4.2 | 208 | 0.53 | | |

[a] The isomer shifts are reported relative to room temperature α-iron foil.

the observed spectra do show some structure which may result from either a quadrupole interaction at the iron site or a distribution of site environments. If fit with a quadrupole doublet, the 295 K spectral parameters given in Table 4 are obtained, parameters that are all very similar to those obtained[13] for a variety of $[Cp_2Fe]^+$-containing compounds.

At 78 and 4.2 K, the spectra of **2** are broadened as is shown in Figure 4. The broadening results from slow paramagnetic relaxation on the Mössbauer time scale of the unpaired electrons present in these paramagnetic compounds.[16] The resulting average effective paramagnetic hyperfine fields have been estimated by fitting the spectra either with a magnetic sextet or with a sextet and a singlet or doublet. Thus, the resulting average effective paramagnetic hyperfine fields, which are given in Table 4, are only a first approximation. Future work will include the fitting of these spectra as a function of temperature with a paramagnetic relaxation model.

**Magnetic Susceptibility Measurements.** The temperature dependence of the product of the magnetic susceptibility with temperature, $\chi T$, for compound **2** is shown in Figure 5. The variation of $\chi T$ is almost independent of temperature with an average value of 0.80 $cm^3$ K $mol^{-1}$. This large deviation from the spin-only value of 0.375 $cm^3$ K $mol^{-1}$ is in agreement with literature data reported for various ferrocenium salts[17,18] and is attributed to spin−orbit coupling combined with a low-symmetry crystal field distortion on the $^2E_{2g}$-$(a_{1g}{}^2e_{2g}{}^3)$ ground state of the ferrocenium ion.[17] The slight decrease in $\chi T$ observed at low temperature (0.71 $cm^3$ K $mol^{-1}$ at 6 K) suggests weak intermolecular antiferromagnetic interactions between the ferrocenium centers in agreement with Mössbauer spectra studies (see above). Indeed, because of the steric hindrance of the mesogenic fragment, the ferrocenium magnetic centers are not expected to interact strongly. No significant changes were noticed during the melting process. The observed slight decrease in the 390−410 K temperature range is mainly due to a decentering of the sample associated with a volume contraction in the sample holder, a contraction that is almost compensated for upon re-centering the sample at the end of the heating process (at 410 K).

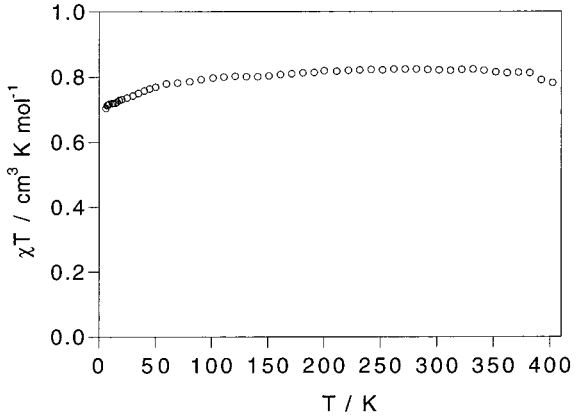


**Figure 5.** Temperature dependence of the product of the magnetic susceptibility with temperature for **2**.

Possible correlations between the magnetic and mesomorphic properties, a through magnetic-field-induced orientation of the magnetic centers that have the required anisotropy,[19] have also been investigated. No significant change has been observed in the magnetic susceptibility when the sample was cooled from the isotropic fluid (410 K) into the columnar liquid-crystalline phase: superimposable heating and cooling curves were obtained (not shown). This may be due to the low anisotropy of the ferrocenium associated with the effect of the bulky organic substituents, substituents that do not permit strong intermolecular interactions, but do favor disorientation.

(16) Hoy, G. R. In *Mössbauer Spectroscopy Applied to Inorganic Chemistry*; Long, G., Ed.; Plenum Press: New York, 1984; Vol. 1, p 195.

(17) (a) Sohn, Y. S.; Hendrickson, D. N.; Gray, H. B. *J. Am. Chem. Soc.* **1970**, *92*, 3233. (b) Hendrickson, D. N.; Sohn, Y. S.; Gray, H. B. *Inorg. Chem.* **1971**, *10*, 1559. (c) Maki, A. H.; Berry, T. E. *J. Am. Chem. Soc.* **1965**, *87*, 4437. (d) Robbins, J. L.; Edelstein, N.; Spencer, B.; Smart, J. C. *J. Am. Chem. Soc.* **1982**, *104*, 1882.

(18) Broderick, W. E.; Thompson, J. A.; Godfrey, M. R.; Sabat, M.; Hoffman, B. M. *J. Am. Chem. Soc.* **1989**, *111*, 7656.

(19) (a) Galyametdinov, Yu.; Athanassopoulou, M. A.; Griesar, K.; Kharitonova, O.; Soto-Bustamante, E. A.; Tinchurina, L.; Ovchinnikov, I.; Haase, W. *Chem. Mater.* **1996**, *8*, 922. (b) Bikchantaev, I.; Galyametdinov, Yu.; Prosvirin, A.; Griesar, K.; Soto-Bustamante, E. A.; Haase, W. *Liq. Cryst.* **1995**, *18*, 231.

## Conclusions

The above results, in conjuction with those we have already reported for **I** and **II**,[1] prove that the ferrocene−ferrocenium couple is a valuable system for preparing redox-active liquid-crystalline switches: first, the nature of the liquid-crystalline phases can be tuned (**1** and **2**, switching mode between isotropic and columnar phases; **I** and **II**, switching mode between isotropic and smectic phases[1]) by means of synthesis at the organometallic level, and second, the Mössbauer and magnetic characteristics observed for **1** and **2** are similar to those of the parent ferrocene and ferrocenium species. This result is of fundamental importance because it shows that grafting of a mesogenic group onto ferrocene or ferrocenium ion does not alter the remarkable features of these entities. The design of switchable anisotropic materials that combine the unique properties of ferrocene and ferrocenium with liquid-crystalline features, such as their fluidity and organization, has become feasible.

## Experimental Section

**Materials.** THF (sodium, benzophenone, under $N_2$) and $CH_2Cl_2$ ($P_2O_5$, under $N_2$) were distilled prior to use. (4-Carboxybutyl)triphenylphosphonium bromide (Fluka, 99%), $^t$-BuOK (Fluka, 99%), *N*,*N*′-dicyclohexylcarbodiimide (Fluka, 99%), silver toluene-4-sulfonate (Fluka, 96%), 4-pyrrolidinopyridine (Aldrich, 98%), and acetone (Fluka, puriss p.a.) were used as received. Nonamethylferrocene carboxaldehyde (**3**),[7] 4-benzyloxy-4′-hydroxybiphenyl,[8] and 4-octadecyloxybenzoic acid[9] were prepared following literature procedures. All the reactions were carried out at room temperature.

**Techniques.** Column chromatography used silica gel 60 (0.060−0.200 mm, SDS). Melting points (uncorrected) were determined on a Büchi 530 instrument. Transition temperatures (onset point) and enthalpies were determined with a Mettler DSC 30 differential scanning calorimeter connected to a Mettler TA 4000 processor, under $N_2$, at a rate of 10 °C/min; Mettler TA72.2/0.5 Graphware was used for treatment of the data. Optical studies were made using a Zeiss-Axioscop polarizing microscope equipped with a Linkam-THMS-600 variable-temperature stage, under $N_2$. $^1$H and $^{13}$C NMR spectra were recorded on a Varian Gemini 200 spectrometer or a Bruker AMX 400 with the solvent as an internal standard. Elemental analyses were done by Mikroelementaranalytisches Laboratorium ETH-Zurich.

**X-ray Diffraction Studies.** Compound **2** was introduced into a Lindemann glass tube of about 0.7 mm in diameter. As the sample decomposed in the temperature range of the liquid-crystalline phase, the exposure times were limited by using Synchrotron radiation (D43 at LURE, Orsay, France) and an imaging plate detector. The wavelength was 1.45 Å and the sample-to-detector distance 390 mm; an evacuated tube was placed between the sample and the detector in order to reduce the scattering background.

**Mössbauer Spectroscopy.** The Mössbauer spectra were obtained between 4.2 and 295 K on a constant-acceleration spectrometer that used a room-temperature rhodium matrix cobalt-57 source and was calibrated at room temperature with α-iron foil. The absorber thicknesses ranged from 75 to 100 mg/cm$^2$, and the resulting spectra have been fit with a quadrupole doublet or, in some cases, with an added sextet. Four spectral measurements at 295 K on three different spectrometers with two separate preparations of $(Me_5Cp)_2Fe$ indicate that its isomer shift, quadrupole splitting, and linewidth are reproducible to ±0.004, ±0.02, and ±0.01 mm/s, respectively. The accuracy for the remaining compounds should be similar. The absolute spectral absorption areas are reproducible to ±0.5%, and as a consequence, the effective recoil masses are valid to ca. ±10 g/mol and the effective Mössbauer temperatures are valid to ca. ±5 K.

**Magnetic Measurements.** The temperature dependence of the magnetic susceptibility was measured using a SHE superconducting SQUID magnetometer in a field of 0.5 T. The sample was first heated from 6 to 410 K (isotropic melt) and then cooled into the columnar phase. The data were corrected for the magnetization of the aluminum sample holder, and the magnetic susceptibility was corrected for the diamagnetism of the constituent atoms using Pascal constants.

**Abbreviations.** *N*,*N*′-Dicyclohexylcarbodiimide = DCC; column chromatography = CC.

**Synthesis. Compound 4.** To a suspension of (4-carboxybutyl)triphenylphosphonium bromide (8.91 g, 20.10 mmol) in THF (35 mL) (under $N_2$) was added dropwise a solution of potassium *tert*-butoxide (5.63 g, 50.17 mmol) in THF (30 mL). The mixture was stirred for 20 min, and a solution of nonamethylferrocene carboxaldehyde (**3**) (3.42 g, 10.05 mmol) in THF (30 mL) was added dropwise. The mixture was stirred for 3 h and concentrated to dryness. To the solid residue was added diethyl ether and a 5 N NaOH aqueous solution (**3** is soluble in diethyl ether; **4** is soluble in the alkaline solution). The layers were separated, and the aqueous phase was acidified with a 2 N HCl aqueous solution to acidic pH. Then, AcOEt was added. The organic layer was recovered, dried ($MgSO_4$), and evaporated to dryness. Purification of the solid residue by CC (hexane/acetone, 2:1) gave pure **4** (3.57 g, 84%). Mp = 120 °C. $^1$H NMR (200 MHz, acetone-$d_6$): δ 6.05 (d, 1 H, CH=), 5.8−5.6 (m, 1 H, CH=), 2.38 (t, 2 H, $CH_2CO_2$), 2.19 (m, 2 H, C=C$CH_2$), 1.79 (m, 2 H, C$H_2CH_2CO_2$), 1.74 (s, 6 H, $CH_3$), 1.65 (s, 6 H, $CH_3$), 1.59 (s, 15 H, $CH_3$). Anal. Calcd for $C_{25}H_{36}O_2Fe$ (424.41): C, 70.75; H, 8.55. Found: C, 70.53; H, 8.54.

**Compound 5.** To a mixture of **4** (3.57 g, 8.41 mmol), 4-benzyloxy-4′-hydroxybiphenyl (2.79 g, 10.10 mmol), DCC (2.08 g, 10.08 mmol), and $CH_2Cl_2$ (140 mL) was added 4-pyrrolidinopyridine (0.26 g, 1.75 mmol). The mixture was stirred for 3 h and evaporated to dryness. Purification of the solid residue by CC ($CH_2Cl_2$/$Et_3N$, 100:1) gave pure **5** (4.42 g, 77%). Mp = 132 °C. $^1$H NMR (200 MHz, acetone-$d_6$): δ 7.65−7.33 (m, 9 H, aromatic protons), 7.17 (d, 2 H, aromatic protons), 7.11 (d, 2 H, aromatic protons), 6.11 (d, 1 H, CH=), 5.8−5.7 (m, 1 H, CH=), 5.19 (s, 2 H, C$H_2$Ph), 2.69 (t, 2 H, $CH_2CO_2$), 2.29 (m, 2 H, C=C$CH_2$), 1.90 (m, 2 H, C$H_2CH_2CO_2$), 1.76 (s, 6 H, $CH_3$), 1.66 (s, 6 H, $CH_3$), 1.60 (s, 15 H, $CH_3$). Anal. Calcd for $C_{44}H_{50}O_3Fe$ (682.73): C, 77.41; H, 7.38. Found: C, 77.44; H, 7.36.

**Compound 6.** A mixture of **5** (2.26 g, 3.31 mmol), Pd-(10%)/C (0.22 g), and $CH_2Cl_2$ (80 mL) was stirred under 4 bar of $H_2$ for 18 h. The mixture was filtered and the solvent evaporated to dryness. Purification of the solid residue by CC (first with $CH_2Cl_2$/$Et_3N$, 100:1, to recover unreacted **5**, and then with acetone) and crystallization (EtOH) gave pure **6** (1.53 g, 78%). Mp = 181 °C. $^1$H NMR (200 MHz, acetone-$d_6$): δ 7.60 (d, 2 H, aromatic protons), 7.50 (d, 2 H, aromatic protons), 7.12 (d, 2 H, aromatic protons), 6.93 (d, 2 H, aromatic protons), 2.58 (t, 2 H, $CH_2CO_2$), 2.21 (t, 2 H, $CpCH_2$), 1.8−1.6 [3 × s (27 H, $CH_3$) and 1 m (C$H_2CH_2CO_2$)], 1.5−1.2 (m, 6 H, $CH_2$). Anal. Calcd for $C_{37}H_{46}O_3Fe$ (594.62): C, 74.74; H, 7.80. Found: C, 74.33; H, 7.88.

**Compound 1.** A solution of **6** (180 mg, 0.303 mmol), 4-octadecyloxybenzoic acid (118 mg, 0.302 mol), DCC (62 mg, 0.300 mmol), and 4-pyrrolidinopyridine (catalytic amount) in $CH_2Cl_2$ (20 mL) was stirred for 6 h under $N_2$, filtered, and evaporated to dryness. Purification of the solid residue by CC ($CH_2Cl_2$/$Et_3N$, 98:2) and crystallization (acetone) gave pure **1** (202 mg, 69%). $^1$H NMR (200 MHz, $CDCl_3$): δ 8.17 (d, 2 H, aromatic protons), 7.60 (d, 2 H, aromatic protons), 7.59 (d, 2 H, aromatic protons), 7.28 (d, 2 H, aromatic protons), 7.15 (d, 2 H, aromatic protons), 6.99 (d, 2 H, aromatic protons), 4.06

(t, 2 H, $OCH_2$), 2.58 (t, 2 H, $CH_2CO_2$), 2.06 (t, 2 H, $CpCH_2$), 1.9−1.2 [3 × s (27 H, $CH_3$) and 1 × m (38 H, $CH_2$)], 0.89 (t, 3 H, $CH_3$). $^{13}C$ NMR (100 MHz, $CDCl_3$): $\delta$ 172.20, 164.85, 163.50, 150.49, 150.11, 138.01, 137.89, 132.22, 128.02, 122.07, 121.83, 121.35, 114.22, 82.67, 78.77, 78.60, 78.08, 68.23, 34.24, 31.88, 30.57, 29.66, 29.55, 29.52, 29.32, 29.18, 29.04, 25.93, 25.04, 24.91, 22.64, 14.08, 9.42, 9.39. Anal. Calcd for $C_{62}H_{86}O_5Fe$ (967.21): C, 76.99; H, 8.96. Found: C, 77.11; H, 9.07.

**Compound 2.** To a solution of **1** (120 mg, 0.124 mmol) in $CH_2Cl_2$/acetone (10 mL, 1:1) was added dropwise a solution of silver toluene-4-sulfonate (35 mg, 0.125 mmol) in acetone (10 mL). The mixture was stirred for 5 min, filtered over Celite, and evaporated to dryness. Purification of the solid residue by CC (first with $CH_2Cl_2$/MeOH, 98:2, to recover unreacted **1**, and then with a gradient of $CH_2Cl_2$/MeOH, 98:2 → 90:10) and crystallization (acetone/AcOEt) gave pure **2** (110 mg, 78%). Anal. Calcd for $C_{69}H_{93}O_8SFe$ (1138.40): C, 72.80; H, 8.23; S, 2.82. Found: C, 72.76; H, 8.27; S, 2.89.

**Acknowledgment.** R.D. acknowledges the Swiss National Science Foundation for financial support. G.J.L. thanks Drs. O. A. Pringle and P. C. Ezekwenna and Mr. R. Rossow for experimental help in obtaining the Mössbauer spectra; this research was supported in part by the U.S. National Science Foundation through a Division of Materials Research Grant No. 95-21739. D.L. acknowledges the Commissariat à l'Energie Atomique (CEA), the C.N.R.S., and the TMR research network 3MD (ERBFMRXCT980181) from the European Community for financial support.

OM9905308